Diamond turning of micro-lens array on the roller featuring high aspect ratio

Peng Huang[a,b], Suet To[b], Zhiwei Zhu[b,c,*]

[a] College of Mechatronics and Control Engineering, Shenzhen University, Shenzhen 518060, China

[b] State Key Laboratory of Ultra-precision Machining Technology, Department of Industrial and Systems Engineering, The Hong Kong Polytechnic University, Kowloon, Hong Kong SAR, China

[c] School of Mechanical Engineering, Nanjing University of Science and Technology, Nanjing, 210094 J.S., China

* Corresponding author: E-mail:zw.zhu@njust.edu.cn (Z. Zhu)

Abstract:

Slow slide servo (S^3) assisted diamond turning combining roll-to-roll replication has been extensively regarded as a very promising technique for the generation of micro-lens arrays (MLAs) for optical applications. However, to avoid undesired interference between the flank surface of the tool and the machined structure, the aspect ratio (AR) (ratio of height to aperture) of machined MLAs is usually restricted to be very small as for the diamond turning process. To generate MLAs with high AR on the roller, a new method is proposed to increase the practical clearance angle during turning by lowering the position of the cutting tool tip in vertical direction. The optimal tool path determination algorithm is developed with full consideration of tool radius as well as tool position. Effectiveness of the proposed method is demonstrated well experimentally through turning a MLA with AR of 0.158 (79 μm height to 500 μm aperture).

Keywords: Ultra-precision diamond turning; Slow slide servo; Micro-lens array; High aspect ratio

1. Introduction

Freeform optical surfaces have been extensively used for decades in a variety of fields, including bio-medicine, defense and astronomy. Micro-lens arrays (MLAs), a special kind of freeform surfaces, have been widely applied to both imaging and non-imaging systems because of their fantastic features such as wide fields of view, large depth of field and high sensitivity to motions [1-6]. To generate MLAs, many techniques have been developed, including lithography related processes [7], laser direct-writing [8], mechanical broaching [9], diamond milling [10] and fast-/slow slide servo diamond turning [11], etc..

Among all those methods, slow slide servo (S^3) diamond turning is a very promising method with high efficiency, high accuracy and high flexibility for the fabrication of MLAs [11, 12]. To massively produce MLAs for optical applications, the roll-to-roll replication has been usually employed by adopting MLA molds generated from S^3 diamond turning. To optimize the S^3 based generation of MLAs on both rollers and end-faces, effects of cutting conditions [13], tool geometry [14], tool path generation strategy [15], system dynamics [16] and error motions [17] on the surface generation have been comprehensively investigated in the current state-of-the-art studies to achieve submicron form accuracy and nanometric surface roughness. To overcome some inherent defects in S^3 turning, and accordingly to achieve uniform surface quality, a novel end-fly-cutting-servo technique has also been developed based on the basic S^3 technique to achieve large-scale generation of MLAs [3].

Although a lot of efforts have been devoted to the fabrication of MLA through S^3 turning, the aspect ratio (AR) (ratio of height to aperture) of the machined lenslet is

usually restricted to be very small due to the limited clearance angle of typical diamond tools [11, 16]. It is noteworthy that diamond milling technique can be employed to generate MLAs with high AR, but with the limitations of low machining efficiency and low flexibility to shapes of the lenslets.

In order to fabricate MLAs on rollers with high AR, the current study proposes a new method through lowering the position of the cutting tool tip (CTT) in the vertical direction. The details of the principle of this method as well as the corresponding tool path generation algorithm are presented in the section 2. The proposed method is verified by a cutting experiment in the section 3, and the results are discussed in the section 4. Finally, the main conclusion is drawn in the section 5.

2. Machining method

2.1 Principle of the machining method

Employing a diamond tool to cut MLAs, an important issue to be considered is the interference between the to-be-machined surface and the flank surface of the diamond tool. The relationship between the geometries of the tool and the to-be-machined surface is illustrated in Fig. 1. P_t is the point at the tool tip, and P_m is the point on the to-be-machined surface which is away from P_t in the opposite direction of cutting. The distance between the CTT and the back of the diamond tool is denoted by B as shown in Fig. 1.As for the point$P_i$which is an arbitrary point between P_t and P_m on the to-be-machined surface, and the angle between $\overrightarrow{P_tP_i}$ and the cutting direction is ϕ_i. For the cut of each lenslet, the angle ϕ_i must be smaller than the clearance angle

γ of the diamond tool to avoid the undesired interference. This leads to a limited AR of the machined MLA for a given diamond tool.

Figure 2 (a) shows the configuration of the tool and workpiece for the conventional S^3 turning of MLAs on the roller. The center lines of both the roller and the CTT are in the same horizontal plane. In this case, the AR is directly dependent on the nominal clearance angle γ of the diamond tool. To obtain high AR using the same diamond tool, the practical clearance angle should be enlarged through tuning the cutting direction. Basing on this concept, the clearance angle is increased by lowering the position of the CTT in the vertical direction. Compared with ordinary cutting, an extra-angle of α is obtained between the cutting direction and the tool flank surface as shown in Fig. 2 (b). In general, the angle is highly dependent on the relative distance between the CTT and the central line of the spindle in the vertical direction, which can be expressed by

$$\alpha = \arcsin(\frac{d}{R}) \tag{1}$$

where R is the radius of the roller.

Therefore, the practical clearance angle during cutting can be determined by

$$\gamma_{eq} = \alpha + \gamma \tag{2}$$

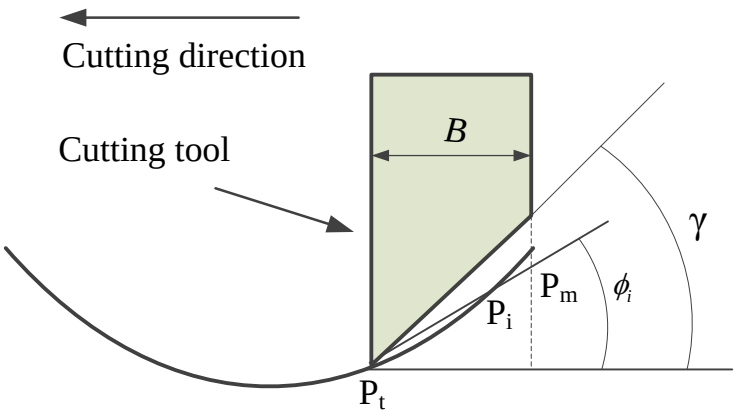

Fig. 1 Schematic of interference between the cutting tool and the machined surface

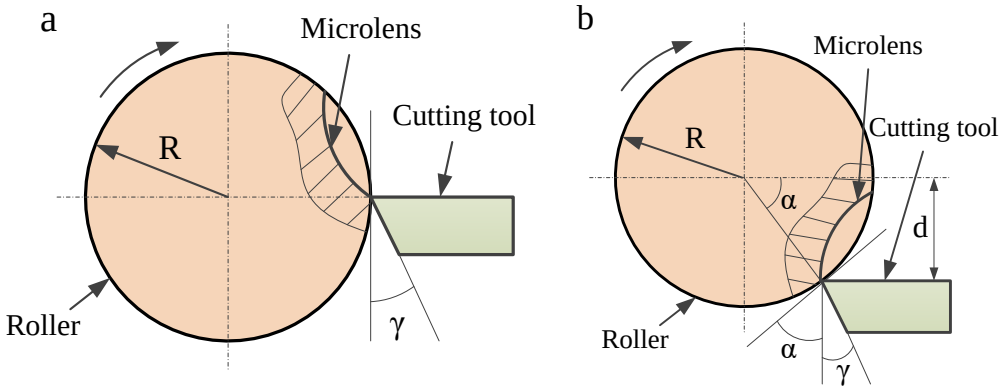

Fig. 2 Schematic of machining methods: a) the ordinary method, and b) the proposed method.

2.2 The optimal tool path determination

2.2.1 Description of MLA on the roller

With the evenly distributed MLA on the roller, the interval between any two adjacent lenslets is a in both circumferential and axial direction of the roller as shown in Fig. 3. O_R-$X_R Y_R Z_R$ is fixed as static and defined as the reference Cartesian coordinate system, and the $O_R Z_R$ axis is consistent with the rotational axis of the roller. A planar lenslet can be expressed in its Cartesian coordinate system O_P-UVW as $w = f(u,v)$. Following the transfer relationship in Fig. 4, a lenslet on the roller in the cylindrical coordinate system (ρ, ϕ, z) can be mapped to a planar lenslet in the Cartesian coordinate system O_P-UVW by:

$$\begin{cases} u = -(\mathrm{mod}(\dfrac{z}{a}) + \dfrac{a}{2}) \\ v = \mathrm{mod}(\dfrac{R\phi}{a}) - \dfrac{a}{2} \\ w = \rho - R \end{cases} \tag{3}$$

where $\mathrm{mod}(\cdot)$ is the operator for taking the remainder, and the coordinate system *O-XYZ* is attached on the roller and concurrently rotates with it. Meanwhile, the Z-axis is consistent with the corresponding rotational axis.

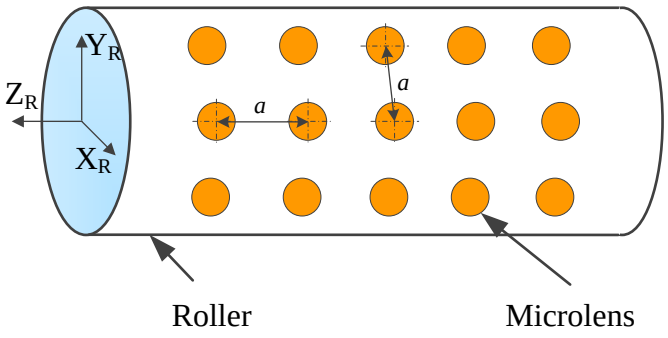

Fig. 3 Schematic of MLA on the roller

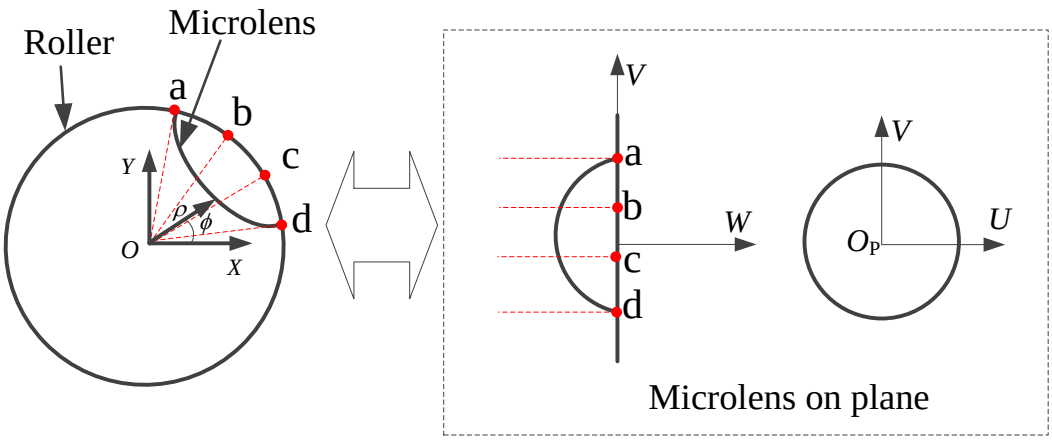

Fig. 4 Relationship between positions of a MLA on the roller and on a planar surface

2.2.2 Determination of the actual CTT coordinates

In the current study, the cutting tool moves alone the axial direction of the roller with

a feed rate of f_z, and the spindle synchronously rotates, generating a spiral toolpath between the tool and the roller. The rotational angle of the spindle is evenly discretized into N points. Therefore, the rotation angle of the k-th cutting point in the tool path can be expressed by:

$$\theta_k = 2\pi \frac{k-1}{N} \tag{4}$$

The corresponding axial coordinate of the cutting tool in the reference system O_R-$X_R Y_R Z_R$ of the roller can be expressed by:

$${}^{R}z_k = -\frac{k-1}{N} f_z \tag{5}$$

The relative position between the diamond tool and the roller is illustrated in Fig. 5. With the k-th cutting point, the relatively moved distance of the tool on the roller along the circumferential direction can be obtained as:

$$l_k = R\theta_k \tag{6}$$

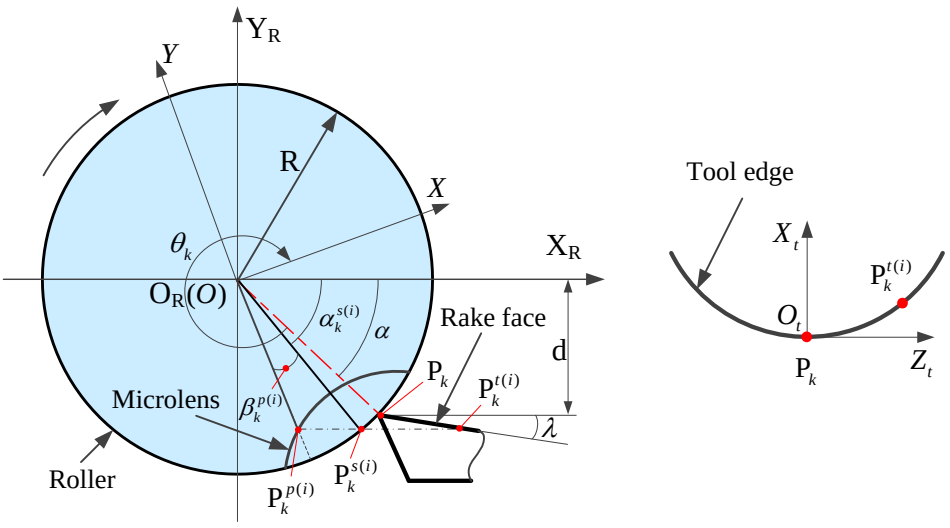

Fig. 5 Relative position between the diamond tool and the roller

As shown in Fig. 5, the initial coordinates of the CTT P_k on the roller surface can be determined in the O_{R}-$X_{\mathrm{R}}Y_{\mathrm{R}}Z_{\mathrm{R}}$ system by:

$$\begin{cases} {}^{R}x_k = R\cos\alpha \\ {}^{R}y_k = -d \\ {}^{R}z_k = {}^{R}z_k \end{cases} \tag{7}$$

The initial position of the OX axis of the fixed coordinate system *O*-*XYZ* coincides with the line $\overline{O_R P_k}$. Recall Eq. (3), the coordinates of the point P_k can be mapped to the O_{P}-*UVW* system of a planar lenslet by:

$$\begin{cases} u_k = -(\mathrm{mod}(\dfrac{z_k}{a}) + \dfrac{a}{2}) \\ v_k = \mathrm{mod}(\dfrac{l_k}{a}) - \dfrac{a}{2} \\ w_k = 0 \end{cases} \tag{8}$$

For any discrete point $\mathrm{P}_k^{t(i)}$ on the tool edge, its coordinates in the fixed tool coordinate system O_{t}-$X_{\mathrm{t}}Y_{\mathrm{t}}Z_{\mathrm{t}}$ are $({}^{t}x^{t(i)}, {}^{t}y^{t(i)}, {}^{t}z^{t(i)})$. Its coordinates $({}^{R}x_k^{t(i)}, {}^{R}y_k^{t(i)}, {}^{R}z_k^{t(i)})$ in the O_{R}-$X_{\mathrm{R}}Y_{\mathrm{R}}Z_{\mathrm{R}}$ then can be determined by:

$$\begin{vmatrix} {}^{R}x_k^{t(i)} \\ {}^{R}y_k^{t(i)} \\ {}^{R}z_k^{t(i)} \\ 1 \end{vmatrix} = T_k \cdot \begin{vmatrix} {}^{t}x^{t(i)} \\ {}^{t}y^{t(i)} \\ {}^{t}z^{t(i)} \\ 1 \end{vmatrix} \tag{9}$$

where T_k is a position transition matrix expressed by

$$T_k = \begin{vmatrix} \cos\lambda & -\sin\lambda & 0 & {}^{R}x_k \\ \sin\lambda & \cos\lambda & 0 & {}^{R}y_k \\ 0 & 0 & 1 & {}^{R}z_k \\ 0 & 0 & 0 & 1 \end{vmatrix} \tag{10}$$

Assume $\mathrm{P}_k^{s(i)}$ is the projected point of the tip point $\mathrm{P}_k^{t(i)}$ on the cylindrical roller surface, the coordinates of the point $\mathrm{P}_k^{s(i)}$ in the O_{P}-UVW system can be expressed by:

$$\begin{cases} u_k^{s(i)} = -(\mathrm{mod}(\dfrac{{}^{R}z_k^{t(i)}}{a}) + \dfrac{a}{2}) \\ v_k^{s(i)} = \mathrm{mod}(\dfrac{l_k^{s(i)}}{a}) - \dfrac{a}{2} \\ w_k^{s(i)} = 0 \end{cases} \tag{11}$$

where

$$l_k^{s(i)} = R\alpha_k^{s(i)} \tag{12}$$

$$\alpha_k^{s(i)} = \arcsin(\frac{-{}^{R}y_k^{t(i)}}{R}) \tag{13}$$

Assuming the projected point of $\mathrm{P}_k^{t(i)}$ on the desired surface is $\mathrm{P}_k^{p(i)}$, its coordinates in the reference coordinate system O_{R}-$X_{\mathrm{R}}Y_{\mathrm{R}}Z_{\mathrm{R}}$ can be determined based on two different cases.

Case 1:

If $\sqrt{(u_k^{s(i)})^2 + (v_k^{s(i)})^2} > D_{aperture}/2$, where $D_{aperture}$ is the aperture of the lenslet, the coordinates of $\mathrm{P}_k^{p(i)}$ in the reference coordinate system O_{R}-$X_{\mathrm{R}}Y_{\mathrm{R}}Z_{\mathrm{R}}$ can be determined by:

$$\begin{cases} {}^{R}x_k^{p(i)} = \sqrt{R^2 - ({}^{R}y_k^{t(i)})^2} \\ {}^{R}y_k^{p(i)} = {}^{R}y_k^{t(i)} \\ {}^{R}z_k^{p(i)} = {}^{R}z_k^{t(i)} \end{cases} \tag{14}$$

Case 2:

If $\sqrt{(u_k^{s(i)})^2+(v_k^{s(i)})^2} \le D_{aperture}/2$, the coordinates $(u_k^{p(i)}, v_k^{p(i)}, w_k^{p(i)})$ of the point $\mathrm{P}_k^{p(i)}$ in the O_P-UVW system can be obtained as:

$$\begin{cases} u_k^{p(i)} = u_k^{s(i)} \\ \sin(\alpha_k^{s(i)} + \beta_k^{p(i)}) = \dfrac{-{}^R y_k^{t(i)}}{R + w_k^{p(i)}} \\ w_k^{p(i)} = f(u_k^{p(i)}, v_k^{p(i)}) \end{cases} \tag{15}$$

Then the related coordinates of $\mathrm{P}_k^{p(i)}$ in reference coordinate system O_R-$X_\mathrm{R}Y_\mathrm{R}Z_\mathrm{R}$ are:

$$\begin{cases} {}^R x_k^{p(i)} = \sqrt{(R + w_k^{p(i)})^2 - ({}^R y_k^{t(i)})^2} \\ {}^R y_k^{p(i)} = {}^R y_k^{t(i)} \\ {}^R z_k^{p(i)} = {}^R z_k^{t(i)} \end{cases} \tag{16}$$

By compensating the tool nose radius, the actual coordinates of the CTT which can be equivalently regarded as the coordinates of the point in the toolpath is determined by:

$$\begin{cases} {}^R x_k^a = {}^R x_k - \min\left\{ \left\| \overrightarrow{O_R P_k^{p(i)}} - \overrightarrow{O_R P_k^{t(i)}} \right\|_{i=1,\ldots,m} \right\} \\ {}^R y_k^a = {}^R y_k \\ {}^R z_k^a = {}^R z_k \end{cases} \tag{17}$$

where m is the number of discrete points of the tool edge.

3. Experimental setup

To verify the proposed turning method, a cutting experiment was conducted on an ultra-precision machine tool (Moore Nanotech 350FG). The specification of the

machine tool is summarized in Table 1. A diamond cutting tool with clearance angle of 7° was utilized. The experimental setup is graphically shown in Fig. 6. After the cutting, the machined MLA was measured with an optical surface profiler (Zygo@ Nexview) to obtain the three dimensional topography of the machined lenslet.

Table 1. Information of the machine tool and the workpiece

Straightness error in critical direction	X axis: 0.3 μm over full travel; Z axis: 0.3 μm over full travel;
Spindle motion accuracy	Axial: ≤12.5 nm; Radial: ≤12.5 nm;
Spindle position accuracy Workpiece	± 1.0 arc seconds (compensated)
material	Brass

With the cutting process, the specified cutting conditions and tool geometry are summarized in Table 2. Radius of the spherical lenslet and the interval between any two adjacent lenslets were 0.435862 mm and 0.6 mm respectively. The AR of each lenslet based on the proposed method in the current experiment was 0.158 (79 μm height to 500 μm aperture). By means of the same diamond tool, the cross-sectional profile with ultimate AR based on the conventional method is illustrated in Fig. 7, which is only about 0.03 (15 μm height to 500 μm aperture). Evidently, the AR generated by the proposed method is significantly enlarged by adopting the proposed turning method.

Table2. Cutting conditions and cutting tool geometry

Radius of workpiece R	16.35 mm
Lowered distance d	8.905 mm
Feedrate f_z	5 μm/rev

Rotational division number N	3600
Tool nose radius r_t	0.1 mm
Tool clearance angle γ	7°
Nominal tool rake angle α_t	0°

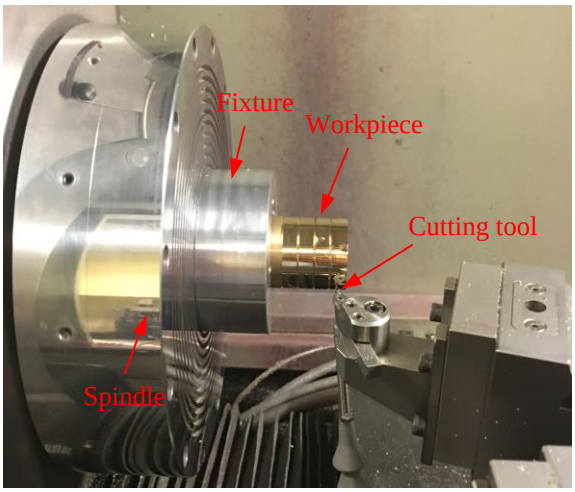

Fig. 6 Experimental setup for the cutting process

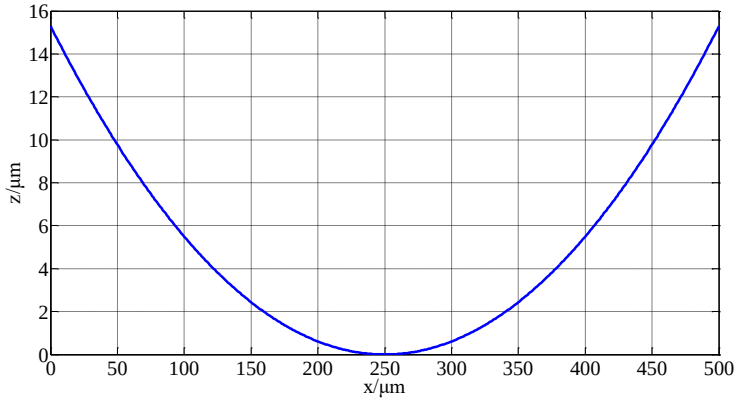

Fig. 7 The lenslet profile with ultimate AR based on conventional method

4. Results and discussion

The measured 3-D topography of an arbitrary lenslet in the MLA is shown in Fig. 8 (a), appearing to have no distortions. From the profiles shown in Fig. 8 (b) and Fig. 8 (c), the cross-sectional profiles in both cutting and feed directions exhibit good agreement with the desired profile, indicating that the interference between the diamond tool and the machined surface does not happen. The machining error is mainly in the range of several hundred nanometers for most part of the machined

profile, showing good machining accuracy. On the other aspect, significant fluctuation with large amplitude of several micrometers can be observed at the beginning of the machined profile along the cutting direction, whereas only little fluctuation can be found along the feed direction. By removing the designed spherical substrate, the fluctuation marks in the cutting direction can be seen on the 3-D residual topography of the machined lenslet as shown in Fig. 9. The difference between the feed direction and cutting direction is due to the large acceleration and deceleration of servo system of machine tool in the cutting direction, which is a common problem for the fabrication of MLA with STS diamond turning [3,9,18].

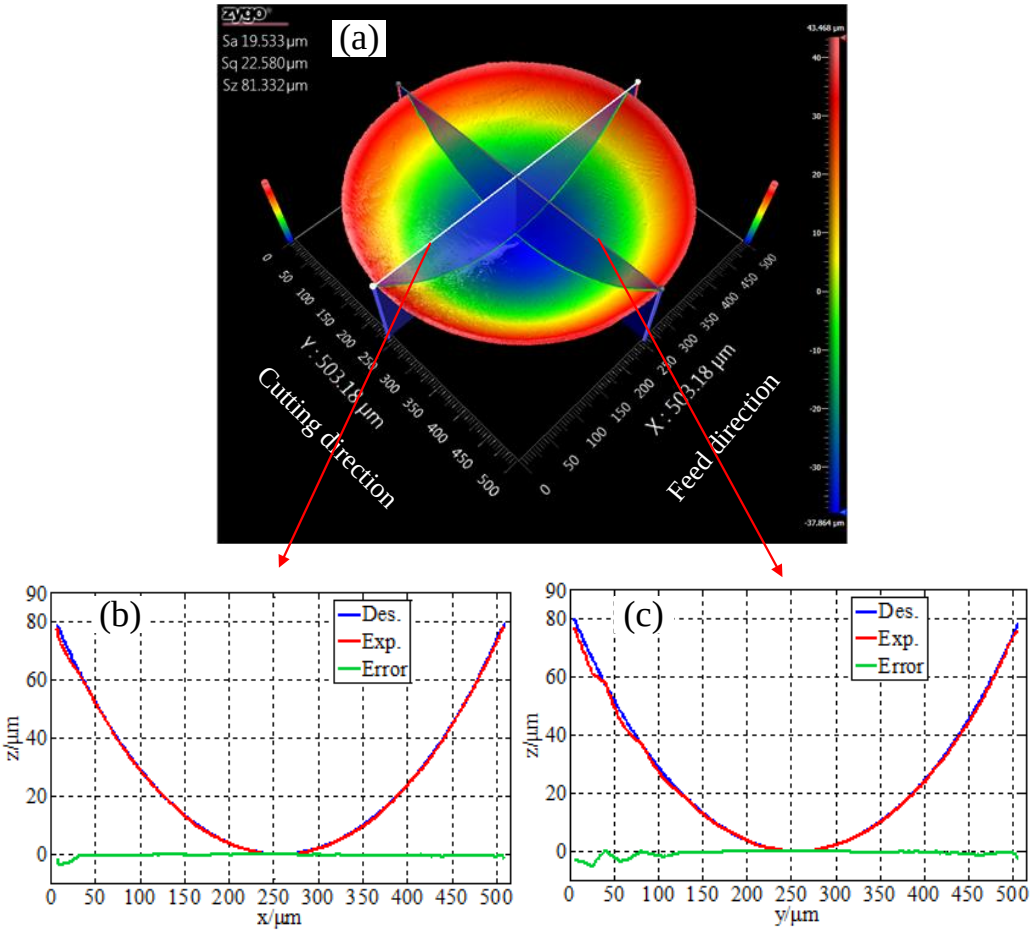

Fig. 8 (a) topography of machined lenslet, (b) profile in feed direction, (c) profile in cutting direction

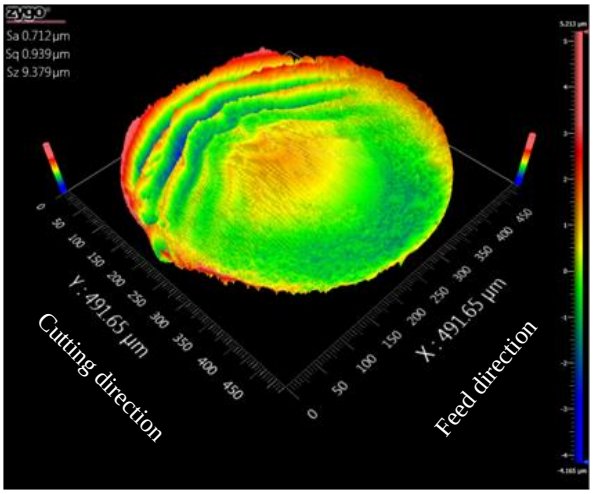

Fig. 9 Topography of machined lenslet by removing the substrate

5. Conclusions

Derived from the basic slow slide servo technique, a new machining method is proposed to generate MLAs with high AR on the roller in the current study. In this method, the position of the CTT in the vertical direction is set to be much lower than that used in the conventional turning. This leads to a much larger clearance angle in turning, accordingly to effectively avoid interference between the cutting tool and machined surface when turning MLAs with high AR.

Experimental turning of a MLA was conducted to verify the proposed method. The AR of machined lenslet in this experiment reaches to about 0.158 (79 µm height to 500 µm aperture), which is significantly larger than the ultimate AR of about 0.03 (15 µm height to 500 µm aperture) in conventional turning with the same diamond tool. High form accuracy without distortions was observed on the obtained lenslet, demonstrating that the interference between the diamond tool and machined surface can be avoided well when adopting the proposed turning method.

Acknowledgments

This work described in this paper was jointly supported by the National Natural Science Foundation of China (51675455, 51705254), Natural Science Foundation of SZU (2017036), Natural Science Foundation of Jiangsu Province (BK20170836), and Fundamental Research Funds for the Central Universities (30917011301, 309171A8804).

References:

[1] Song YM, Xie Y, Malyarchuk V, Xiao J, Jung I, Choi KJ, Li R (2013) Digital cameras with designs inspired by the arthropod eye. Nature 497(7447): 95-99.

[2] Zhang X, Fang F, Yu L, Jiang L, Guo Y (2013) Slow slide servo turning of compound eye lens. Optical Engineering 52(2):023401.

[3] Zhu Z, To S, Zhang S (2015) Large-scale fabrication of micro-lens array by novel end-fly-cutting-servo diamond machining. Optics Express 23(16): 20593-20604.

[4] Lee XH, Moreno I, Sun CC (2013) High-performance LED street lighting using microlens arrays. Optics Express 21(9): 10612-10621.

[5] Li L, Allen YY (2010) Development of a 3D artificial compound eye. Optics Express 18(17): 18125-18137.

[6] Jeong KH, Kim J, Lee LP (2006) Biologically inspired artificial compound eyes. Science 312(5773): 557-561.

[7] Radtke D, Duparré J, Zeitner UD, Tünnermann A (2007) Laser lithographic fabrication and characterization of a spherical artificial compound eye. Optics express 15(6):3067-3077.

[8] Wang T, Yu W, Li C, Zhang H, Xu Z, Lu Z, Sun Q (2012) Biomimetic compound eye with a high numerical aperture and anti-reflective nanostructures on curved surfaces. Optics letters 37(12): 2397-2399.

[9] Li L, Allen YY (2012) Design and fabrication of a freeform microlens array for a compact large-field-of-view compound-eye camera. Applied optics 51(12): 1843-1852.

[10] Scheiding S, Allen YY, Gebhardt A, Loose R, Li L, Risse S, Tünnermann A (2011) Diamond milling or turning for the fabrication of micro lens arrays: comparing different diamond machining technologies. In SPIE MOEMS-MEMS, International Society for Optics and Photonics (pp. 79270N-79270N).

[11] Zhang X, Fang F, Yu L, Jiang L, Guo Y (2013) Slow slide servo turning of compound eye lens. Optical Engineering 52(2): 023401.

[12] Zhang H, Li L, McCray DL, Scheiding S, Naples NJ, Gebhardt A, Allen YY (2013) Development of a low cost high precision three-layer 3D artificial compound eye. Optics express 21(19):22232-45.

[13] Yu DP, San Wong Y, Hong GS (2011) Optimal selection of machining parameters

for fast tool servo diamond turning. The International Journal of Advanced Manufacturing Technology 57(1-4):85-99.

[14] Fang FZ, Zhang XD, Hu XT (2008) Cylindrical coordinate machining of optical freeform surfaces. Optics Express 16(10): 7323-7329.

[15] Yu DP, Gan SW, San Wong Y, Hong GS, Rahman M, Yao J (2012) Optimized tool path generation for fast tool servo diamond turning of micro-structured surfaces. The International Journal of Advanced Manufacturing Technology 63(9-12): 1137-1152.

[16] Zhu Z, To S, Zhu W-L, Huang P (2017). Feasibility study of the novel quasi-elliptical tool servo for vibration suppression in the turning of micro-lens arrays. International Journal of Machine Tools and Manufacture 122: 98-105.

[17] Liu X, Zhang X, Fang F, Zeng Z, Gao H, Hu X (2015). Influence of machining errors on form errors of microlens arrays in ultra-precision turning. International Journal of Machine Tools and Manufacture, 96, 80-93.

[18] Zhou M, Zhang HJ, Chen SJ (2010) Study on diamond cutting of nonrationally symmetric microstructured surfaces with fast tool servo. Materials and Manufacturing Processes 25(6):488-494.